Progress In Electromagnetics Research M, Vol. 73, 131–139, 2018

Research on Spatial Characteristics of Wireless Channel in the Mine Tunnel

Min Gao, Yu Huo*, and Yaqiang Zheng

Abstract—Mining and mineral exploration are very important in the global economy. In mining operations, communication systems play vital roles in ensuring personal safety, enhancing operational efficiency and process optimization. Multiple Input Multiple Output (MIMO) systems have been widely used in the mine environment to suppress the multi-path problem of the tunnel and enhance the capacity of the channel. In order to realize the optimal performance of MIMO system, spatial characteristics of wireless signal in an underground tunnel must be considered. In this paper, the wave propagation model combined with the modal theory and ray theory is used to simulate mine underground wireless channel. Meanwhile, the theoretical models of the signal Angular Power Spectrum (APS) and Angular Spread (AS) are constructed. After simulation and comparison, the following conclusions can be drawn: the APS distribution of the wireless signal is similar to the Gaussian distribution; the position of the antenna in the cross section of the mine tunnel has a small influence on the signal AS, which can be neglected; the roughness of the mine tunnel wall can change the characteristic of the signal AS to some extent.

1. INTRODUCTION

In order to achieve high-efficiency production, risk avoidance and disaster monitoring, the application of wireless network is urgently needed in mine construction and production [1, 2]. However, underground wireless signal transmission is mainly limited by the inner wall of the mine tunnel, and its multi-path fading is more prominent than the ground environment. Moreover, the multi-path fading seriously affects the reliability and effectiveness of wireless network link transmission [3, 4]. In recent years, the research and application of underground MIMO system have been used to overcome multi-path constraints [5–7]. In order to achieve the optimal performance of the MIMO system, it is necessary to understand the spatial distribution characteristics in the wireless environment [6, 7], including the Angular Power Spectrum (APS) and Angular Spread (AS). However, the research on the spatial distribution characteristics of underground wireless signals is still limited.

In [6], the frequency response of the wireless channel is measured in an arched subway tunnel with a width of 8.6 m and a height of 6.1 m. Then, the power distribution and angle of the wireless signal in the azimuth angle are indirectly obtained by using the virtual array method and the channel estimation method. However, the application of this method is limited and the data obtained by this approach is not accurate. In [8], the signal received power is only tested as the width and height of the mine tunnel section changes. A spatial fading of signal along the roadway was tested in a rectangular-like mine, but the statistical characteristics of spatial fading and parameter analysis of measured results are not shown in [9]. Compared with the measuring method, the theoretical method can perfectly identify each propagation path. In [7], the multi-wave mode waveguide model and geometrical optics model are

Received 2 July 2018, Accepted 7 September 2018, Scheduled 19 September 2018

* Corresponding author: Yu Huo (gm@htc.edu.cn).

The authors are with the School of Mechanical and Electrical Engineering, Hefei Technology College, IOT Research Center for Mine, China University of Mining and Technology, Hefei 238000, China.

respectively used to calculate the characteristics of the azimuth angular spread of the wireless signal in a smooth-wall mine tunnel with the propagation distance. The radiation field distribution characteristics of a half-wave dipole antenna in a rectangular roadway were simulated using waveguide theory in [10–12].

In this paper, the modal theory and ray theory are combined to improve the spatial distribution theory of underground wireless channels and get the theoretical expression of APS. An underground wireless channel model is constructed by the combined theory to better guide the design and application of MIMO systems. On this basis, the influence of the roughness of the tunnel wall on the frequency characteristics of the signal AS is simulated and analyzed, and at the same time, the effect of the antenna at different positions in the tunnel wall also be simulated.

2. THEORETICAL ANALYSIS

2.1. Combined Model

Wave propagation model combined with the modal theory and ray theory, referred to as a combined model in the following has been developed and used by Huo et al. [13] to characterize wireless propagation inside tunnels. Similar to previous waveguide-based models, in this model, tunnels are considered to be over-sized dielectric waveguides. Similar to previous ray-based models, in this model, each mode in a tunnel can also be determined approximately by a ray. The properties which distinguish this method from earlier models are as follows: (1) the ray tracing is simplified and corrected by the restrictions of the guided wave modes; (2) it provides a complete signal power transmission formula from the transmitter to the receiver without dealing with the initial field intensity on the excitation plane; (3) by considering all the possible propagation modes in the tunnel, the signal attenuation can be described as a continuous process for the whole propagation zone of the tunnel, and there is no need to consider any breakpoints.

For the model proposed in [13], the construction and processing method can be summarized into the following steps:

(1) According to the restrictions of the propagation modes which are possible to exist in a tunnel from the modal theory, determine the emitting quantity and direction of all possible rays.

(2) Calculate the reflection number, the traveling distance, the relative received power, the arriving angle, the arriving position and other parameters of each possible ray by ray approach.

(3) Decide whether a ray hits the receiver or not by the reception spheres method.

In order to verify the correctness of the combined model, the combined model was constructed and simulated to compare with measured data.

Set up a Cartesian coordinate system in the mine tunnel. The x, y, and z axes are along the width, height, and length of the mine tunnel, respectively. The origin is located at the center of the roadway cross section. The width of the rectangle tunnel is w and the height is h. The receiver is located at the front of the transmitter and is arranged along the z-axis.

The angles of departure of the ray corresponding to the (m, n) mode and marked as i are characterized by the azimuth angle φ_{Di} and elevation θ_{Di} respectively, as follows [13]:

$$\begin{aligned} \varphi_{Di} &= \frac{\pi}{2} \pm \arcsin\left(\frac{m}{w\sqrt{4/\lambda^2 - n^2/h^2}}\right) \\ \theta_{Di} &= \frac{\pi}{2} \pm \arcsin\left(\frac{n\lambda}{2h}\right) \end{aligned} \tag{1}$$

where m, n are the order of the propagation wave mode [14], $m = 1, ..., [2w/\lambda]$, $n = 1, ..., [2h/\lambda]$, and λ is the wavelength of the electromagnetic wave.

If the antenna is bidirectional, the number M of the rays excited in the tunnel is given by

$$M = 2\frac{4w}{\lambda} \cdot \frac{4h}{\lambda} \tag{2}$$

According to Geometrical Optical theory [15], the relative power of the ith ray when it travels to the receiving plane (which depends on the receiver location)

$$a_i = \frac{\lambda}{4\pi} \frac{\sqrt{G_i} R_1^{(i)} R_2^{(i)} \exp\left(-j\frac{2\pi}{\lambda} r_i\right)}{r_i} \tag{3}$$

G_i is the antenna gains of the ith ray. R_1^i and R_2^i are the Fresnel reflectance from the vertical walls and the horizontal walls, respectively.

The predicted received signal power at the coordinate (x, y, z) is given by

$$p = \left| \sum_{i}^{M} \delta_i a_i \right|^2 \tag{4}$$

If the ith ray is effectively received, $\delta_i = 1$; otherwise, $\delta_i = 0$.

Verification of the combined approach with experimental work performed in [16, Fig. 18] is given in Fig. 1(b). For the verification, the tunnel is an equivalent rectangle of 5.3 m height and 7.8 m wide, and the transmitting and receiving antennas are half-wave vertically polarized vertical dipoles antennas. Two antennas are placed at the same height (2 m) and horizontal positions of one-quarter of the tunnel width. The electromagnetic wave with frequency characteristics of 450 MHz and 900 MHz is simulated and tested. At 450 MHz, half-wave dipoles are used. In the case of 900 MHz, wide-band horn antennas are used, and the gain of which is 7 dBi. The simulated and measured results are shown in Fig. 1. The curve in Fig. 1 shows the relation of signal receiving power with transmission distance, and we can conclude that the results calculated by the combined approach are consistent with the measured results. For the case of 450 MHz, the average error between the theoretical data obtained by the combined method and the measured data is 3.59 dBm, and the mean square error is 4.35 dBm. Similarly, the average error and mean square error calculated at 450 MHz are 1.32 dBm and 6.98 dBm. Besides, by comparing the results with the conventional ray approach in Fig. 1(a), it can be seen that the ray method gets corrected by considering the restrictions from modal theory.

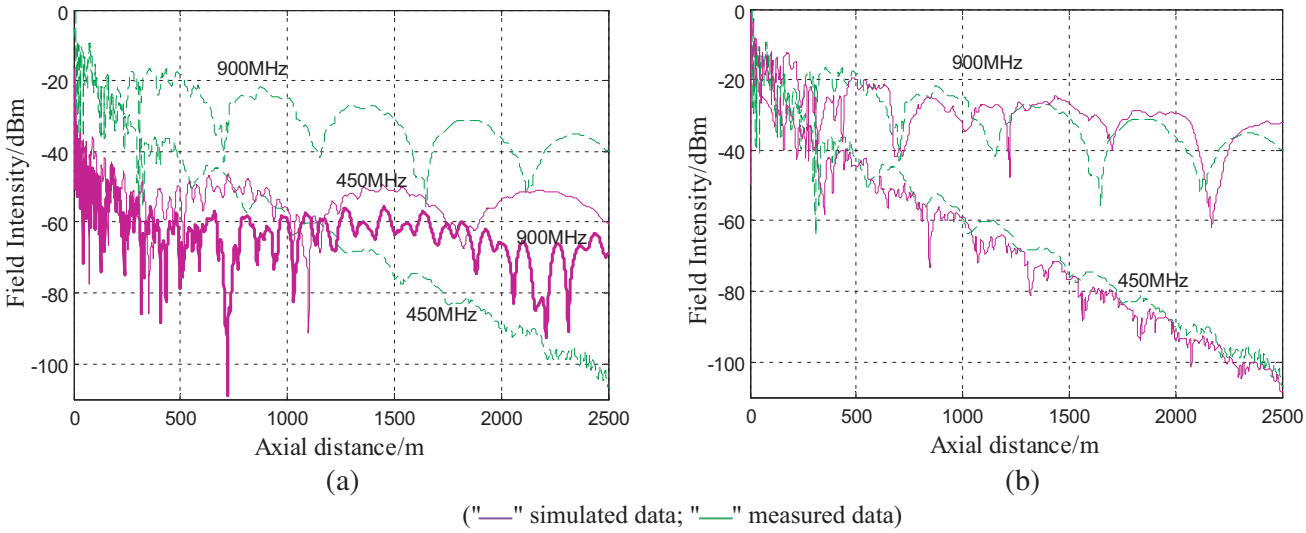

Figure 1. (a) The simulation data obtained by ray method and the measured data. (b) The simulation data obtained by combined approach and the measured data.

2.2. Angular Power Spectrum

At a certain time t, certain azimuth φ and elevation θ, the impulse response of the wireless channel can be defined as follows:

$$h(t, \theta, \varphi) = \sum_{i=1}^{M} a_i \delta_i \delta[t - \tau_i] \delta[\theta - \theta_{ri}] \delta[\varphi - \varphi_{ri}] \tag{5}$$

where τ_i represents the delay of the ith distinguishable path; φ_i and θ_i are the angle of the arrival direction of the ith path, respectively. Illustrated in Fig. 2–Fig. 4 in [13], φ_i and θ_i can be deduced as

$$\varphi_i = \begin{cases} \pi + \phi_D, & N_1 \text{ is even} \\ 2\pi - \phi_D, & N_1 \text{ is odd} \end{cases} \quad \theta_i = \begin{cases} \pi - \theta_D, & N_2 \text{ is even} \\ \theta_D, & N_2 \text{ is odd} \end{cases} \tag{6}$$

where N_1 is the total number of reflections on the tunnel vertical walls of the ith ray, and N_2 is the total number of reflections on the tunnel horizontal walls of the ith ray.

Based on the impulse response of the channel in Eq. (6), the received power $p(\varphi, \theta)$ of the signal $s(t)$ along the azimuth φ and elevation θ directions can be obtained as follows:

$$p(\varphi, \theta) = \left| \sum_i a_i s(\varphi - \varphi_i, \theta - \theta_i) \right|^2 \tag{7}$$

The received power $p(\varphi)$ of the signal along the azimuth φ direction is calculated by the following formula

$$p(\varphi) = \left| \sum_i a_i s(\varphi - \varphi_i) \right|^2 \tag{8}$$

The received power $p(\theta)$ of the signal along the elevation θ direction is calculated by the following formula

$$p(\theta) = \left| \sum_i a_i s(\theta - \theta_i) \right|^2 \tag{9}$$

The mean azimuth of the signal is denoted by $\bar{\varphi}$, and the mean elevation of the signal is denoted by $\bar{\theta}$. Through the statistical analysis of angular power spectrum in Eqs. (8) and (9), the formula is given as follows:

$$\overline{\varphi} = E\{\varphi\} \tag{10}$$

$$\overline{\theta} = E\{\theta\} \tag{11}$$

where $E\{\cdot\}$ is the mathematical expectation function.

The azimuth AS of the signal is denoted by σ_φ, and the elevation AS is denoted by σ_θ. Through statistical analysis of angular power spectrum in Eqs. (8) and (9), the formula is given as follows:

$$\sigma_\varphi = \sqrt{E\{\varphi^2\} - [E\{\varphi\}]^2} \tag{12}$$

$$\sigma_\theta = \sqrt{E\{\theta^2\} - [E\{\theta\}]^2} \tag{13}$$

3. SIMULATION ANALYSIS

3.1. Comparison with Experimental Measurements

In [9], the spatial fading of a 450 MHz wave signal is measured in a rectangular-shaped mine with a width of 5 m and a height of 6 m. Moreover, the electrical parameters of the test tunnel wall is a complex number, and the roughness of the tunnel wall is characterized by the standard deviation of the average transverse dimensions in [9]. Therefore, the wall electrical parameters of the test roadway is set to

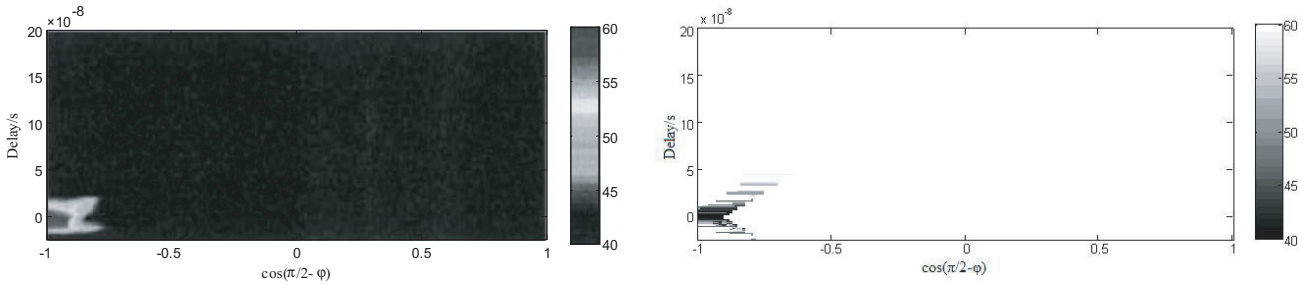

(a) (b)

Figure 2. The spatial fading of a 450 MHz wave signal in a rectangular-shaped mine. (a) Measured results; (b) Theoretical results.

$5 - j0.01$, and the roughness of the roadway is set to 0.5 m. The transceiver antenna is a vertically polarized half-wave dipole antenna, and the test distance is 40 m. The measured results are shown in Fig. 2(a). The abscissa is the cosine of the angle ($|\pi/2 - \varphi|$) between the signal arrival direction and the longitudinal axis of the roadway. The ordinate is the relative delay between each resolution path and the first arrival path. Gray scale is signal strength, and the unit is dB. According to this measured condition, in this paper, we also carry out this simulation based on the combined model. The simulation results are shown in Fig. 2(b). Compared with Fig. 2(a) and Fig. 2(b), the simulation is basically the same, and the model is verified.

3.2. Spatial Characteristics of Wireless Channel

APS of the wireless channel should be a complex function related to the parameters of the roadway wall, the geometry of the roadway, the carrier frequency, and the antenna position. This section firstly analyzes the statistical distribution of signal power along the AOA in a rectangular roadway, and then calculates the influence of each parameter on AS. In our simulation setups, we consider a kind of common lane size in Chinese mines, which is rectangular tunnel with a height of 3 m and width of 4 m. The wall of the tunnel is composed of coal-rock media with an electrical parameter of $10 - j0.18$. The wireless signal center frequency in the tunnel is 900 MHz. Two horizontally polarized omnidirectional antennas are used as receiving and transmitting antennas respectively, and the antennas are placed in the center of the tunnel. The distance between the receiving antenna and the transmitting antenna is 100 m.

3.2.1. Characterization of APS

Normalizing the maximum received power, the received power versus the AOA is computed, and the simulated results are shown in Fig. 3. $\bar{\varphi} = 270°$, $\bar{\theta} = 90°$ are the average angle of arrival of the received signal, AS is $\sigma_\varphi = 2.22°$, $\sigma_\theta = 5.80°$. At present, the distribution function of uniform distribution, $\cos^n$ distribution, Laplacian distribution and Gaussian distribution are commonly used to describe descriptive signal APS. For the power space distribution curve, shown in Fig. 3(a), it is obvious that the APS in the roadway does not conform to the uniform distribution. For the $\cos^n$ distribution, the value of n decreases exponentially as the AS decreases. Therefore, when the value of AS is less than 10° the value of n can reach more than 100 orders of magnitude and in this case, and the $\cos^n$ distribution is very close to the Gaussian distribution [17]. In this paper, the calculated data mainly used to compare and fit with Laplacian and Gaussian function.

Through data fitting, the wireless signal APS in the roadway has been modeled by a Laplacian

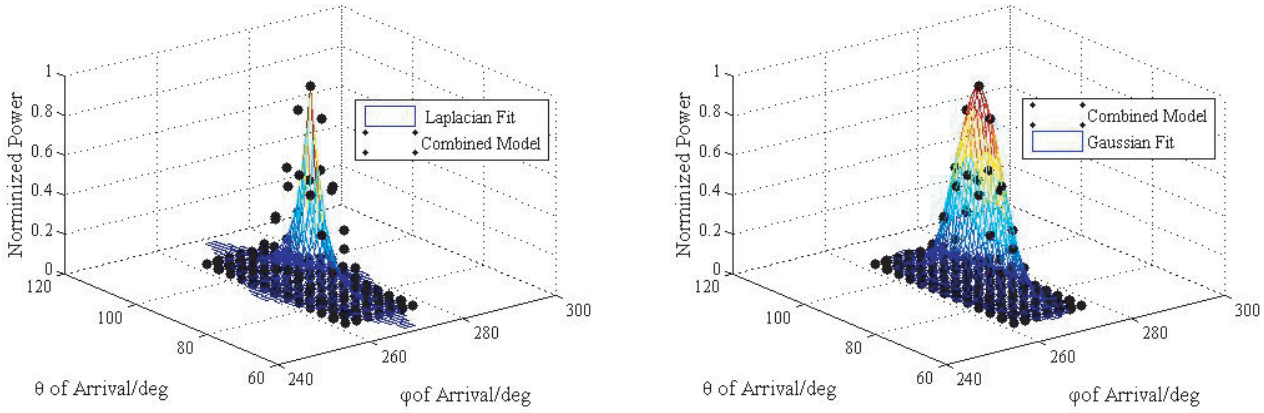

Figure 3. Comparison of APS for the rectangular tunnel. (a) Laplacian fit of the APS for the tunnel. (b) Gaussian fit of the APS for the tunnel.

function as follows [18]:

$$p_{\text{Laplacian}}(\varphi,\theta)=\frac{1}{2\sigma_\varphi\sigma_\theta}\exp\left(-\frac{\sqrt{2}\,|\varphi-\overline{\varphi}|}{\sigma_\varphi}\right)\cdot\exp\left(-\frac{\sqrt{2}\,|\theta-\overline{\theta}|}{\sigma_\theta}\right)G(\varphi,\theta) \tag{14}$$

The calculated data is compared with the Laplacian function as shown in Fig. 3(a).

Through data fitting, the wireless signal APS in the roadway has been modeled by a Gaussian function as follows [19]:

$$p(\varphi,\theta)=\frac{1}{2\pi\sigma_\varphi\sigma_\theta}\exp\left[-\frac{1}{2}\left(\frac{\varphi-\overline{\varphi}}{\sigma_\varphi}\right)^2\right]\cdot\exp\left[-\frac{1}{2}\left(\frac{\theta-\overline{\theta}}{\sigma_\theta}\right)^2\right]G(\varphi,\theta) \tag{15}$$

Similarly, the calculated data are compared with the Gaussian function as shown in Fig. 3(b). In further comparison of Fig. 3(a) and Fig. 3(b), the wireless signal APS distribution in the roadway is similar to the mean ($\bar{\varphi}=270°$, $\bar{\theta}=90°$) Gaussian distribution.

3.2.2. Effect of Carrier Frequency

The trend of the signal AS with the carrier frequency is also calculated in Fig. 4. As shown in Fig. 4, when the carrier frequency is lower than 500 MHz, due to the waveguide characteristics of the roadway, as the frequency increases, a large number of high-order modes break through the limit of the cutoff frequency and are promptly excited, and the propagation loss of each mode is also rapidly reduced [20], then the value of AS showing a rapid growth trend. On the other hand, when the carrier frequency is higher than 500 MHz, the propagation loss of the guided wave mode and the density of the wave mode in the roadway tend to be stable [20], and the value of AS gradually converges.

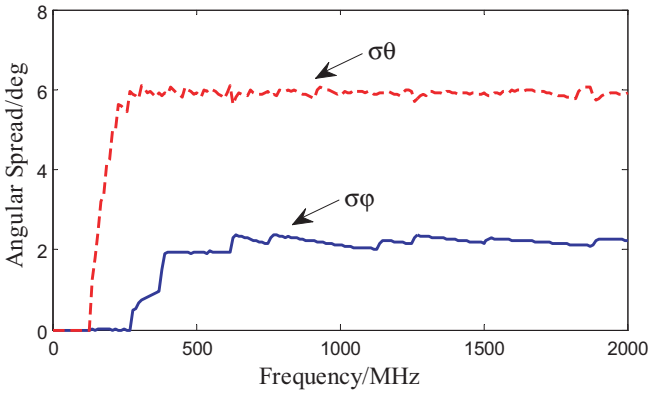

Figure 4. The trend of the signal AS with the carrier frequency.

3.2.3. Effect of Antenna Position

The positions of the antenna, including the longitudinal position and the lateral position in the roadway, all have an important influence on the radiation field coverage of the wireless channel [8, 11]. In Fig. 5, typical lateral positions of the antenna are calculated, such as roadway section center, the middle of the roadway top wall, roadway section corner, and the middle of the roadway right wall. The curve of signal AS with the longitudinal distance of the transmitting and receiving antenna at different positions is calculated and compared. As shown in Fig. 5, with the increase of the distance between the transmitting and receiving antennas, each high-order wave mode is rapidly degraded, and the signal transmission is gradually determined by the lower secondary modes which are closer to the longitudinal axis of the roadway. Therefore, the signal AS first decreases rapidly and then changes slowly. When the antenna is in different positions in the cross section of the roadway, the influence on the signal AS is very small, and the reason for this result is the four-sided symmetrical structure of the roadway.

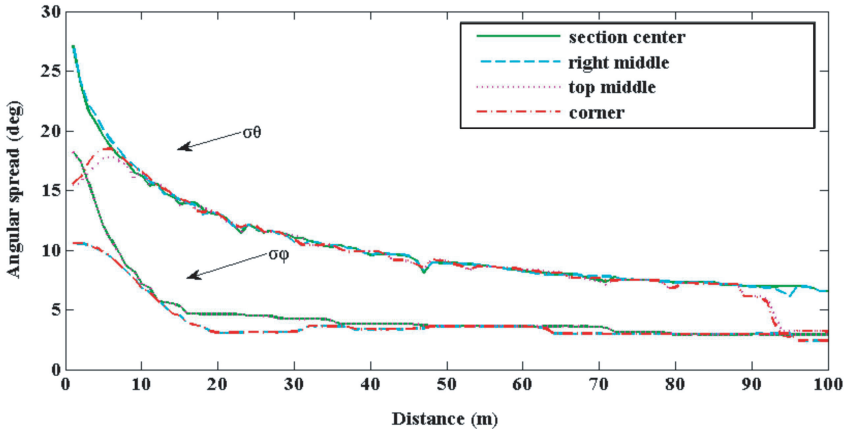

Figure 5. Comparison of four typical lateral positions for characterizing AS in a tunnel.

3.2.4. Effect of Mine Tunnel Wall Parameters

The parameters of the wall, including the dielectric parameters of the wall, the roughness of the roadway wall, and so on, all have effect on the propagation of electromagnetic waves in the tunnel. Among them, the dielectric electrical parameters consist of relative permittivity and conductivity. Moreover, the existing literature has reached a relatively unanimous conclusion that the relative permittivity has an important influence on the propagation characteristics of the channel, and the influence of the conductivity can be neglected in [20, 21]. With regard to the influence of the roughness of the roadway wall, especially on the spatial characteristics of the signal, there is less research on related literature.

Therefore, in this paper more work is focused on the effect of the roughness of the roadway wall on AS. The variation of the angular spread of the wireless signal with the roughness of the roadway wall is shown in Fig. 6. Due to the existence of tunnel wall roughness, when electromagnetic waves are ejected into the tunnel wall, electromagnetic waves are scattered. The scattering loss caused by electromagnetic wave scattering will further increase the propagation loss of the guided wave mode [20, 21]. The greater the roughness of the tunnel wall is, the greater the scattering loss of electromagnetic waves is [20, 21]. When the lower-order mode propagates from the transmitting terminal to the receiving terminal along the longitudinal axis of the roadway, there is basically no reflection or only a few reflections. However, the higher-order mode needs to experience multiple reflections during propagation. Therefore, the tunnel wall roughness has a greater influence on the higher-order mode than the lower-order mode.

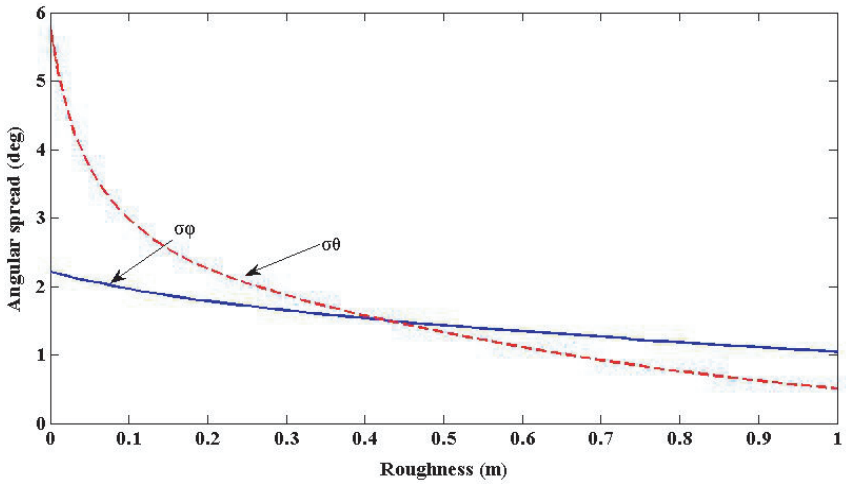

Figure 6. AS with different roughness in a tunnel.

It can be inferred from the above discussion that the greater the roughness of the tunnel wall is, the greater the difference is in propagation loss between the higher-order mode and the lower-order mode. In the propagation process, the higher-order mode plays a smaller role than the lower-order mode. The higher-order mode has a larger grazing angle, which means that the more the received power of the signal is concentrated in the lower-order mode, the smaller the angular spread is.

Therefore, as shown in Fig. 6, AS shows a decreasing trend with increasing roughness. Moreover, the effect from the roughness on elevation AS σ_θ is greater than azimuth AS σ_φ. It makes AS of horizontal polarizations for the tunnel different. When the tunnel walls are smooth and the height of the studied tunnel smaller than its width, σ_θ is larger than σ_φ. However, contributing to the wall roughness, as the value increases enough that it cannot be ignored, σ_θ rapidly decreases and becomes smaller than σ_φ in Fig. 6. This result implies that horizontal polarization is more suitable for MIMO in tunnels with serious wall roughness, while vertical polarization is more suitable in tunnels with smooth walls.

4. CONCLUSION

Multi-antenna technology can use space diversity to increase channel capacity and solve the problem of multi-path interference. In order to adapt to the special electromagnetic environment in coal mines, reasonable multi-antenna structure design and algorithm research cannot be separated from understanding and mastering the spatial characteristics of wireless channels. In this paper, the electromagnetic wave propagation theory of the fusion wave mode and ray is used to simulate the underground mine wireless channel. Based on combining the modal and ray approaches, APS and AS theoretical models of the underground wireless channel are constructed. Compared with the measured data and modal approach, the theoretical model is verified. After the simulation and comparison, the following conclusions can be drawn:

(1) The power spatial distribution of underground wireless signals is similar to the Gaussian distribution;

(2) The signal AS is mainly affected by the longitudinal position of the antenna in the tunnel, while the position of the antenna in the cross section of the mine tunnel has a small influence on the signal AS, which can be neglected;

(3) The presence of roadway wall roughness can change the characteristics of the signal AS. In most tunnels, of which the height is smaller than its width, if the walls are smooth, vertical polarization is more suitable for MIMO, and if the walls are seriously rough, horizontal polarization is more suitable.

ACKNOWLEDGMENT

This work is supported by National Key Research and Development Project No. 2017YFC0804404, Jiangsu Natural Science Fund-Youth Fund No. BK20160264, Anhui Natural Science Research Key Project No. KJ2015A391 and No. KJ2016A663.

REFERENCES

1. Arghavan, E. F., S. Bashir, D. G. Michelson, and S. Noghanian, "A survey of wireless communications and propagation modeling in underground mines," *IEEE Communications Surveys & Tutorials*, Vol. 15, No. 4, 1524–1545, Dec. 2013.
2. Sun, Z., I. F. Akyildiz, and G. P. Hancke, "Capacity and outage analysis of MIMO and cooperative communication systems in underground tunnels," *IEEE Trans. Wireless Communications*, Vol. 10, No. 11, 3793–3803, Nov. 2011.
3. Sun, Z. and I. F. Akyildiz, "Channel modeling and analysis for wireless networks in underground mines and road tunnels," *IEEE Trans. Communications*, Vol. 58, No. 6, 1758–1768, Jun. 2010.
4. Ranjan, A., P. Misra, and H. B. Sahu, "Experimental measurements and channel modeling for wireless communication networks in underground mine environments," *2017 11th European Conference on Antennas and Propagation (EUCAP)*, 1345–1349, 2017.

5. Yin, S. X., D. W. Chen, and Q. Zhang, "Mining spectrum usage data: A large-scale spectrum measurement study," *IEEE Trans. Mobile Computing*, Vol. 11, No. 6, 1033–1046, Jun. 2016.
6. Garcia-Pardo, C., J.-M. Molina-Garcia-Pardo, M. Lienard, D. P. Gaillot, and P. Degauque, "Double directional channel measurements in an arched tunnel and interpretation using ray tracing in a rectangular tunnel," *Progress In Electromagnetics Research M*, Vol. 22, 91–107, 2012.
7. Forooshani, A. E., S. Noghanian, and D. G. Michelson, "Characterization of angular spread in underground tunnels based on the multimode waveguide mode," *IEEE Trans. Communications*, Vol. 62, No. 11, 4126–4133, 2014.
8. Zhang, Y. P. and Y. Hwang, "Characterization of UHF radio propagation channels in tunnel environments for microcellular and personal communications," *IEEE Trans. Veh. Technol.*, Vol. 47, No. 1, 283–296, 1998.
9. Lienard, M. and P. Degauque, "Natural wave propagation in mine environments," *IEEE Antennas Wireless Propag. Lett.*, Vol. 48, 1326–1339, 2000.
10. Sun, J. P. and M. F. Gao, "Research on the radiation characteristics of symmetrical dipole antenna in rectangular tunnel," *Journal of China Coal Society*, Vol. 35, 2121–2124, 2010.
11. Huo, Y., F. X. Liu, and Z. Xu, "Effect of antenna location on radiation field distribution in coal mine tunnels," *International Journal of Coal Science & Technology*, Vol. 38, 715–720, 2013.
12. Huo, Y., H. D. Zheng, Y. J. Huand G. P. Zhang, "Optimum beam index of mine antenna used in rectangular tunnels," *International Journal of Coal Science & Technology*, Vol. 42, 2776–2782, 2017.
13. Huo, Y., Z. Xu, and F. X. Liu, "A wave propagation model combined the modal theory and ray theory in coal mine tunnels," *Chinese Journal of Electronics*, Vol. 41, 110–116, 2013.
14. Laakman, K. and W. Steier, "Waveguides: Characteristics modes of hollow rectangular dielectric waveguides," *Appl. Opt.*, Vol. 15, No. 5, May 1976.
15. Mahmoud, S. F. and J. R. Wait, "Geometrical optical approach for electromagnetic wave propagation in rectangular mine tunnels," *Radio Science*, Vol. 9, 1147–1158, 1974.
16. Dudley, D. G., M. Lienard, S. F. Mahmoud, and P. Degauque, "Wireless propagation in tunnels," *IEEE Antennas Propag. Mag.*, Vol. 49, No. 2, 11–26, Apr. 2007.
17. Lee, W. C. Y., "Effects on correlation between two mobile radio base-station antennas," *IEEE Trans. Veh. Technol.*, Vol. 22, No. 4, 1214–1224, Nov. 1973.
18. Adachi, F., M. T. Feeney, A. G. Williamson, and J. D. Parsons, "Crosscorrelation between the envelopes of 900 MHz signals received at a mobile radio base station site," *IEE Proc. F*, Vol. 133, No. 6, 506–512, 1986.
19. Pedersen, K. I., P. E. Mogensen, and B. H. Fleury, "Power azimuth spectrum in outdoor environments," *Electron. Lett.*, Vol. 33, No. 18, 1583–1584, 1997.
20. Huo, Y., Z. Xu, and H. D. Zheng, "Characteristics of multimode propagation in rectangular tunnels," *Chinese Journal of Radio Science*, Vol. 25, 1225–1230, 2010.
21. Emslie, G. A., L. L. Robert, and P. F. Strong, "Theory of the propagation of UHF radio waves in coal mine tunnels," *IEEE Transactions on Antennas and Propagation*, Vol. 23, 192–205, 1975.